Tomohiko Ishii · Hisanobu Wakita
Kazuyoshi Ogasawara · Yang-Soo Kim
Editors

The DV-Xα Molecular-Orbital Calculation Method

Springer

The DV-Xα Molecular-Orbital Calculation Method

Tomohiko Ishii • Hisanobu Wakita
Kazuyoshi Ogasawara • Yang-Soo Kim
Editors

The DV-Xα Molecular-Orbital Calculation Method

Springer

Editors
Tomohiko Ishii
Department of Advanced Materials Science
Faculty of Engineering
Kagawa University
Takamatsu, Japan

Hisanobu Wakita
Faculty of Science
Fukuoka University
Johnan-ku, Fukuoka, Japan

Kazuyoshi Ogasawara
Department of Chemistry
School of Science and Technology
Kwansei Gakuin University
Hyogo, Japan

Yang-Soo Kim
Korea Basic Science Institute
Suncheon, Republic of Korea

ISBN 978-3-319-11184-1 ISBN 978-3-319-11185-8 (eBook)
DOI 10.1007/978-3-319-11185-8
Springer Cham Heidelberg New York Dordrecht London

Library of Congress Control Number: 2014955357

Printed on acid-free paper

Springer is part of Springer Science+Business Media (www.springer.com)

Foreword

The discrete variational Xα (DV-Xα) molecular orbital calculation method is one of the most versatile methods for estimating the electronic structures of atom-aggregates or clusters in both ground and excited states. It has been used extensively for solid-state chemistry and physics; materials science; and X-ray, electron, IR, Raman, and UV–vis spectroscopy with great success.

To develop the research on this method, the Society for DV-Xα in Japan was established in 1988, and an annual meeting has been held every summer since then. The International Workshops on DV-Xα have been held five times, once each in Hungary (1996), South Korea (1998), Japan (2001), South Korea (2006) and Japan (2008). The Society for DV-Xα in Korea was established in 2010 and has greatly promoted the research activity in Korea since then.

This proceedings, entitled *The DV-Xα Molecular-Orbital Calculation Method* is published in commemoration of the international symposium of the "Sixth International Conference on the DV-Xα Method (DV-Xα 2010) and the 23rd DV-Xα Annual Meeting," held in Daejeon, Korea, at the KBSI (Korean Basic Science Research Institute) on August 4–6 in 2010. This international conference was organized by the Organizing Committee 2010, which consisted of members of the DV-Xα societies in Japan and Korea who aimed to discuss the research on molecules, particles, crystals, glasses, metals, semiconductors, surface, boundary defects from a physics perspective, organic and inorganic chemistry, materials science and many forms of spectroscopy, the theory of DV-Xα, and related experiments and theories.

The international symposium consisted of 3 plenary, 20 invited and 27 poster sessions. Plenary lecturers Prof. Kazuyuki Tatsumi (the president of the IUPAC) talked about Fe/S cluster preparation, Prof. Di Zhang (Shanghai Jio Tong Univ.) about morphogenetic preparation, and Prof. Masahiko Morinaga (Nagoya Univ.) about alloy designing. Over 80 participants studiously discussed the subject of each lecture and eagerly shared ideas and possible future developments for this excellent method.

Finally, the organizing committee of DV-Xα 2010 concluded by publishing a number of important lectures in book-style proceedings for a notable memory

of our activity, a wider understanding of the DV-Xα method, and to receive evaluations from other scientific fields.

To support this international symposium and the publication of this volume, special thanks should be expressed to both DV-Xα societies in Japan and Korea. The financial supporting funds from the JSPS (Japan Society for the Promotion of Sciences) and the KBSI are also acknowledged.

Fukuoka
25 July, 2014

Hisanobu Wakita
Myung-Chul Chang
Tomohiko Ishii
Yang-Soo Kim

Preface

Theoretical and computational sciences have become one of the most exciting areas of research. For example, the Nobel Prize in chemistry in 2013 was awarded to three theoretical chemists, Professors Martin Karplus, Michael Levitt and Arieh Warshel whose works have greatly influenced many scientists and engineers. The activity at the DV-Xα annual meeting to discuss computational sciences has continued for more than 25 years after the establishment of the DV-Xα society in Japan and Korea. The DV-Xα method has been utilized in not only the fundamental sciences such as physics and chemistry but also in a broader range of engineering areas such as metallurgy, material engineering, electricity, amorphous materials, photology, universology, bio-engineering, and pharmacology. This proceedings volume, entitled *The DV-Xα Molecular-Orbital Calculation Method* is published in commemoration of the international symposium of the "Sixth International Conference on the DV-Xα Method (DV-Xα 2010) and The 23rd DV-Xα Annual Meeting" held in Daejeon, KBSI, Korea, in 2010. In this volume there are 14 most powerful and interesting papers reported as recent activities involving the DV-Xα method. Aspects of the fundamental sciences, including details of calculation methods and related programs, fundamental calculation theories and their expressions, and inter-atomic interaction potential and total energy calculations are included. In addition, a material design method which works by means of chemical bonding, discussions of optical properties of certain materials, application examples of dye-sensitized solar cells, innovative applications of water, the creation of an electrode material for lithium secondary batteries, discussions of the lifetimes of positrons, crystal structural optimization techniques, and the mechanisms of the luminescence of metal complexes are also discussed as examples of applications of the DV-Xα method. We are very proud to publish such a high-quality and fruitful

proceedings volume which offers discussions and examples of applications which have progressed in 4 years since the previous DV-Xα international meeting held in 2010.

Takamatsu, Japan — Tomohiko Ishii
Hyogo, Japan — Kazuyoshi Ogasawara
Suncheon, Republic of Korea — Yang-Soo Kim
Fukuoka, Japan — Hisanobu Wakita
22 July 2014

Contents

Part III Applications

Part I
Fundamentals

Chapter 1
The DV-Xα Molecular Orbital Calculation Method and Recent Development

Yoshiyuki Kowada and Kazuyoshi Ogasawara

1.1 Introduction

Recently, theoretical calculation methods are widely applied in many kinds of the material researches according to the outstanding progress of the computational technology. Among them the DV-Xα method has been widely applied to the development and analysis of the organic and inorganic materials since this method has characteristic advantages compared with the other molecular orbital methods. In this chapter, we would like to introduce the development history and the recent progress of this method.

The DV-Xα cluster method is one of the first principle molecular orbital calculation methods based on the Xα method. The Xα method is one of the electronic state calculation methods by the Hatree-Fock-Slater method proposed by J. C. Slater on 1951. This method is applied not only to the electronic state calculation of molecules and atoms, but also to the energy band calculation of solid-state materials. All atomic orbitals in the periodic table were calculated with Hartree-Fock-Slater method by Herman and Skillman on 1963 and the table of the eigen values, wavefunctions and potentials were reported (Herman and Skillman 1963). On 1965, the calculation results of transuranium elements were reported by Liberman, Waber, and Cromer, in which the Dirac equation with Xα potential was used (Liberman et al. 1965). The first application of Xα potential to

Y. Kowada (✉)
Department of Natural Sciences, Hyogo University of Teacher Education,
942-1 Shimokume, Kato-shi, Hyogo 673-1494, Japan
e-mail: ykowada@hyogo-u.ac.jp

K. Ogasawara
Department of Chemistry, School of Science and Technology,
Kwansei Gakuin University, 2-1 Gakuen, Sanda, Hyogo 669-1337, Japan
e-mail: ogasawara@kwansei.ac.jp

T. Ishii et al. (eds.), *The DV-Xα Molecular-Orbital Calculation Method*,
DOI 10.1007/978-3-319-11185-8_1

the molecular orbital theory was the multiple scattering (MS) Xα method developed by K. H. Johnson on 1966 (Johnson 1966).

In the Xα method, the simple notation of the exchange potential, which is proportion to the third power of the electrondensity ρ with the approximation of the free electron model, is used. Furthermore, the parameter α to this equation, shown in Eq. (1.1), is adapted to expanded this approximation to the general atoms and molecules (Slater 1974),

$$V_{XC}(r_{\uparrow}) = -3\alpha\left[\frac{3}{4\pi}\rho_{\uparrow}(r)\right]^{\frac{1}{3}} \tag{1.1}$$

here $\rho_{\uparrow}$ is the density of the up-spin electron, which means that the exchange potential $V_{XC}(r_{\uparrow})$ is the function of only up-spin electron , so that the exchange interaction is observed only between electrons with the same spin. The same equation is obtained for the down-spin electrons. The total electron density is described as $\rho = \rho_{\uparrow} + \rho_{\downarrow}$. Consequently, the Xα method can be considerably shortened the calculation time than those of any other MO methods.

This method is applied not only to the electronic state calculation of molecules and atoms, but also to the energy band calculation of solid-state materials. After Gaspar and Korn, the densities functional method is developed with more restrict theoretical expansions. Essentially the Xα approximation is still good agreement with the density functional method.

D.E. Ellis, A. Rosen, and H. Adachi et al. developed the DV-Xα cluster method at Northwestern University in the 1970s (Ellis et al. 1976; Rosen et al. 1976) There are several characteristic advantages on this method. That is, the discrete-variational method can be numerically solved the Schrödinger equation at the discrete micro-spatial volume on the sample points scattered in three-dimensional space. The evaluation of the elements of Hamiltonian, H_{ij}, and overlap matrices, S_{ij}, are achieved as weighted sums of integrated values at the sample points instead of the conventional Rayleigh-Rits method,

$$S_{ij} = \sum_{k} \omega(r_k)\phi_j^*(r_k)\phi_j(r_k) \tag{1.2}$$

$$H_{ij} = \sum_{k} \omega(r_k)\phi_j^*(r_k)h(r_k)\phi_j(r_k) \tag{1.3}$$

where r_k is one of the total N sample points in the three-dimensional real space and $\omega(r_k)$ is the integration weight or reciprocal of the sample point density at r_k. As the result, the DV-Xα method can calculate the eigenvalues and the eigen functions of molecular orbitals of the cluster models containing any elements in the periodic table. That is the reason why this method is widely applied to the calculation of the electronic states of the various kinds of inorganic materials.

After the initial period of the development of the DV-Xα method, the respective researchers have been modified the original program and added unique ideas.

At present, there are several versions (program sets) in the present, such as the program set named "dvem" developed by D. E. Ellis, "ADF" by Baerends, "DMOL" by Delly. In Japan, Adachi et al. have been hardly developed program set "scat" to the present (Adachi et al. 1978). The Initial version of scat was developed on the mainframe computer in Osaka University and ported to UNIX workstation in early 1990s. In that time, several programs to draw figures in the scat came to work with the graphical interface on the X-window system. The windows PC version was appeared in the middle of 1990s and this version is the most popular in Japan now.

The development of DV-Xα method has been achieved up to the present. The relativistic version, which included relativistic effect with Dirac equation, is developed at the same time with the non-relativistic version by Schrödinger equation. The results with the relativistic version of DV-Xα method were reported in early 1970s (Rosen and Ellis 1974). The relativistic version had been improved and we can use the program set named rscat (Adachi 1977). The rscat is very easy to use because of the same operation scheme with the non-relativistic scat.

By using the DV-Xα method, the eigenvalue and eigen function of each molecular orbital could be obtained accurately for all elements in the periodic table. However, there are still several problems to be solved for further calculation. One of these problems is the many electron interaction, which is necessary to obtain the optical spectra of 3d transition metal ions and 4f rare-earth ions. In 2001, the program named "gemcalc" has been developed by Ogasawara et al., which can include the many electron interactions by the configuration interaction calculations (Ogasawara et al. 2001). They have already reported many papers about the absorption spectra of the rare-earth ions and phosphors (Ishii et al. 2004b; Ogasawara et al. 2005; Watanabe et al. 2006; Toyoshima et al. 2007; Yoshida and Ogasawara 2009). This calculation method, called "DVME method", has been very attractive since it is one of few methods including both many electron interactions and the relativistic effect. Another problem is the total energy calculation of the clusters and molecules. In the DV-Xα method, the numerical eigen function is used and the integration is adopted to obtain the resonance and overlap integrals. The quite small numeric errors of the integrals at the sample points are accumulated and it affects to the total energy. However, there are two different version of total energy calculation program named TESDA and Coulomb and now we can obtain total energy of any cluster models by the DV-Xα method (Kowada et al. 2009a).

In this chapter, we would like to introduce the recent evaluation of the DV-Xα method. The first topic is the electronic state of solid-state electrolyte in which the calculation of moving ions in solid-state materials and total energy of the cluster model (Kowada et al. 2009). The second is the electronic state of the rare-earth ions in phosphate glasses with the calculation of the absorption and fluorescence spectra of the Pr^{3+} and Tb^{3+} ions (Kowada et al. 2009b).

1.2 Total Energy Calculation

Since there are several programs for the energy calculation, among them we use the program Coulomb to obtain the total energy (Kowada et al. 2009a). The calculated energy obtained in the cluster method is the total energy of the local cluster. Then, we called the total energy as local cluster energy (LCE). First we would like to note that the outline of the calculation procedure of the total energy by the program Coulomb. In the DV-Xα cluster method, the molecular orbitals are obtained by the SCC approximation (Adachi et al. 1978). For the energy calculation, the MOs are re-calculated by the Self Consistent Field (SCF) approximation. In the Coulomb, the SCF molecular orbital calculation is achieved in the following procedure. The wave functions of molecular orbitals calculated by the DV-Xα cluster method are used for the basis functions in the SCF calculation.

$$\phi_\ell = \sum_i C_{i\ell}\chi_i \tag{1.4}$$

The electron density ρ(r) is obtained from the molecular orbitals and the Coulomb potentials between two electrons, V_{ee}, are calculated.

$$\rho(r) = \sum f_\ell \phi_\ell^2(r) \tag{1.5}$$

$$V_{ee}(r_1) = \int \frac{\rho(r_2)}{r_{12}} dr_2 \tag{1.6}$$

The eigenvalues and C_{ij} are obtained by following equations.

$$\left(\widetilde{\mathbf{H}} - \widetilde{\varepsilon}\,\widetilde{\mathbf{S}}\right)\widetilde{\mathbf{C}} = 0 \tag{1.7}$$

$$(H)_{ij} = (K.E.)_{ij} + (V_{Ze})_{ij} + (V_{ee})_{ij} + (V_{ex})_{ij} \tag{1.8}$$

$$(K.E.)_{ij} = \int \chi_i(r_1)\left\{-\frac{1}{2}\nabla_1^2\right\}\chi_j(r_1)dr_1 \tag{1.9}$$

$$(V_{Ze})_{ij} = \int \chi_i(r_1)\{\sum_{n=1}^{\infty} \frac{(-Z_V)}{r_{1V}}\}\chi_j(r_1)dr_1 \tag{1.10}$$

$$(V_{ee})_{ij} = \int \chi_i(r_1)\int \frac{\rho(r_2)}{r_{12}} dr_2\, \chi_j(r_1)dr_1 \tag{1.11}$$

$$(V_{ex\uparrow})_{ij} = -3\alpha\left(\frac{3}{4\pi}\right)^{\frac{1}{3}}\int \chi_{i\uparrow}(r_1)(\rho_\uparrow(r_1))^{\frac{1}{3}}\chi_{j\uparrow}(r_1)dr_1 \tag{1.12}$$

After the SCF calculation, the energy of the cluster is calculated.

$$E = E_{K.E.} + E_{ze} + E_{ee} + E_{ex} + E_{zz} \tag{1.13}$$

where $E_{K.E.}$, E_{Ze}, E_{ee}, E_{ex} and E_{ZZ} mean the kinetic energy of the electrons, the energy of the nuclear-electron attraction, the energy of the electron–electron repulsion, the energy of the exchange term, and the energy of the nuclear-nuclear repulsion, respectively. Each energy term is calculated by the weighted sum of the each value on the sample points except E_{ZZ}. In the program Coulomb, there are two major improvements for the energy calculation. The first is the improvement of the estimation of the Coulomb potential. In the DV-Xα molecular calculation, the electron density is calculated as the spherically symmetric charge densities centered on the nuclei of the molecule. In the Coulomb, however, the Coulomb potential is estimated by the electron distribution based on each molecular orbital. The second is the SCF calculation, which makes the molecular orbitals of the lowest energy with the linear combination of the fixed atomic orbitals obtained by the SCC calculation. These improvements give enough accuracy for the total cluster energy. The number of the sample points used in the energy calculation is 2,000 per atom, which is four times larger than that in the chemical bonding analyses, for the enough precision of the wave functions of molecular orbitals.

1.3 Relativistic DVME Method

The detail of this method will be described in another chapter, so that the outline and the estimation of the theoretical fluorescence spectra are noted here. In the DVME method, Slater determinants corresponding to all the possible electronic configurations are constructed using the four-component fully relativistic molecular spinors obtained by the relativistic DV-Xα cluster calculations. Only electrons occupying the molecular spinors mainly composed of Ln-4f states in the grand state are treated explicitly. Then by diagonalization of the many-electron Hamiltonian, the multiplet energies are obtained as eigenvalues and the many-electron wave functions are obtained as linear combination of the Slater determinants. The relativistic many-electron Hamiltonian is expressed as

$$H = \sum_{i=1}^{n} \left[c\alpha \mathbf{p}_i + \beta c^2 - \sum_{\nu} \frac{Z_\nu}{|\mathbf{r}_i - \mathbf{R}_\nu|} + V_0(\mathbf{r}_i) + \sum_{\mu} \frac{Z_\mu^{eff}}{|\mathbf{r}_i - \mathbf{R}_\mu|} \right] + \sum_{i=1}^{n} \sum_{j>i}^{n} \frac{1}{|r_i - r_j|} \tag{1.14}$$

where α, β are the Dirac matrices, c the velocity of light, r_i, p_i the position and the momentum operator of the ith electron, Z_ν and R_ν the charge and position of the νth nucleus, $Z_{\mu\text{eff}}$ and R_μ the effective charge and position of the μth ion outside the model cluster, n the number of explicitly treated electrons. $V_0(r_i)$ is the potential from the remaining electrons (Watanabe and Kamimura 1989).

The oscillator strengths of electric dipole transitions in the absorption spectra are calculated as follows:

$$I_{if} = 2\Delta E \left| \left\langle \Psi_f \left| \sum_k r_k \cdot e \right| \Psi_i \right\rangle \right|^2 \tag{1.15}$$

Ψ_i and Ψ_f are the initial and final states with energies of E_i and E_f, respectively. ΔE is the energy difference between E_i and E_f. In the case of fluorescence spectra, the transition probabilities of electric dipole transitions are obtained by the following equation:

$$I_{if} = 2\Delta E^3 \left| \left\langle \Psi_f \left| \sum_k r_k \cdot e \right| \Psi_i \right\rangle \right|^2 \tag{1.16}$$

In this calculation, the higher energy state is adopted as the initial state of the fluorescence spectra and usually the grand states is the final state. We could obtained the transition probabilities of the fluorescence spectra in the same manner as the absorption spectra.

1.4 Recent Application of the DV-Xα Method

1.4.1 Electronic State of Mobile Li Ions in Super-Ionic Conductors

1.4.1.1 Introduction

Recent 10 years we have investigated the electronic state of the ion movement in the solid-state materials (Kowada et al. 1998, 2000, 2004, 2008a, b, 2009a, b, c; 2010; Imanaka et al. 2000; Araki et al. 2001). Usually the electronic state calculation of moving ions are very difficult to obtain since Born-Oppenheimer approximation is adapted in popular molecular orbital method. The movement of the ions in the solid sate materials, however, are much slower than that of the electrons that contribute to have any interactions with the surrounding ions in the crystal structure. This means the variation of the interactions between the moving ions and the surrounding matrices could be estimated approximately with several model clusters with the different positions of the moving ions.

In these studies, we have paid attentions on the bonding state of the moving ions from the viewpoints of the interactions named covalency and ionicity between the moving ions and the surrounding ions. Thus the covalent bonding of the moving ions should support an important part of the ion movement in the solid-state materials. We would like to introduce the study of the electronic states of the

Li_3N crystal in which the interaction of the moving ions in superionic conducting materials is analyzed. This material is a typical Li ion conductor and has high ionic conductivity. Furthermore the Li and the N ions usually have covalent interactions in the solid-state materials. We also suggest that how useful the DV-Xα method is to get the relationship between the high ionic conductivity and the covalent interactions of the moving cations in these systems.

1.4.1.2 Li_3N Crystal

There are several studies about the high Li ion conductivity of Li_3N crystal by experimental measurements and theoretical calculations (Wahl and Holland 1978; Walker and Catlow 1981; Koyama et al. 2002; Sarnthein et al. 1996). Several experimental studies reported that the Li_3N crystal contained H^+ ion impurities in interstitial positions and they make a certain concentration of the Li ion vacancies. These vacancies are yield on the planes, which contains both Li and N ions, called Li_2N plane. It is reported that the activation energy of the movement of the Li ion on Li_2N planes is 0.004 eV (Sarnthein et al. 1996). In the Li_3N crystal there is the other kind of the Li ions on the planes containing only the Li ions, which connect between the Li_2N planes. This kind of the Li ions hardly moves compared with that on the Li_2N plane. In addition to this, the Li_3N crystal has the anisotropicity in the ionic conductivity and the Li ion conductivity along the c axis is much smaller than those of the a and b axes.

Thus the Li ion can move easily in the Li_2N plane and hardly move in the Li plane. This is something strange from the viewpoint of the chemical bonding. In the Li_2N plane, the moving Li ions might have strong interaction with the N ions compared with those on the Li plane. Generally the larger interaction between the Li and the N ions seems to impose constraints on the fast movement of the Li ion. The experimental results, however, suggest that the fast movement of the Li ions in the Li_3N crystal is not dependent on the smaller interaction between the Li and the N ions. The chemical bonding of the Li ion should contribute to the fast movement of the Li ion in Li_3N crystal.

1.4.1.3 Model Cluster of Mobile Li Ion in Li_3N Crystal

In order to calculate the movement of the Li ion in the Li_3N crystal, several model clusters are constructed by the crystal structure of the Li_3N crystal (Schulz and Thiemann 1979). This crystal is assigned to the space group of $P_{6/mmm}$ and the lattice constants a and c are 3.65 and 3.88 Å, respectively. The schematic diagrams of the model clusters are shown in Fig. 1.1. The Li_3N crystal has layer structure of two kinds of plane structures, the Li_2N and the Li planes. On the Li_2N plane, there are Li and N ions that make hexagons. On the Li plane there are only Li ions that are bonding with the N ions on the Li_2N planes and are bridging between two Li_2N

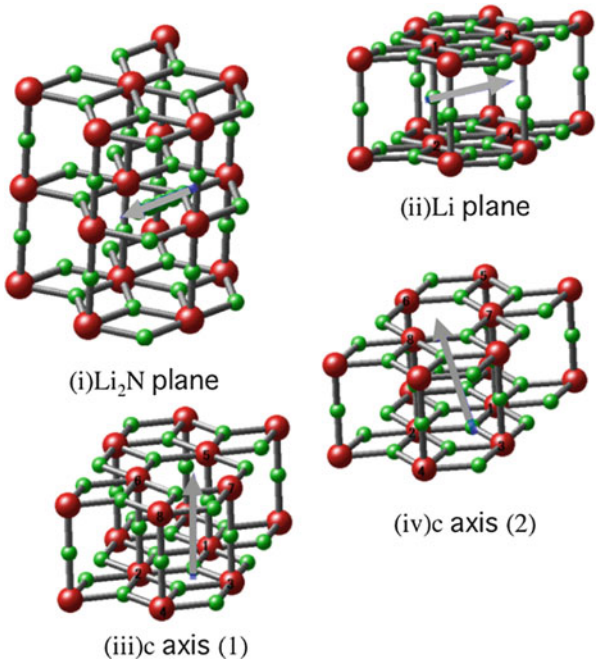

Fig. 1.1 Schematic diagram of the Li_3N model clusters. *Green sphere*: Li ion, *Red sphere*: N ion

planes. The conduction path of the Li ions reported by several experimental studies is included in the Li_2N plane. Figure 1.1 (i) shows the model clusters for the conduction path in Li_2N plane. In this model, one Li ion is removed from the Li_2N plane so that the neighboring Li ion can move to the vacancy. The movement of the Li ion is simulated by using several model clusters with the different positions of the Li ion along the estimated conduction path, since it is fundamentally very difficult to manipulate the movement of the atoms and ions in the molecular orbital calculations. Figure 1.1 (ii) shows the model cluster for the movement of the Li ions on the Li plane. In this model cluster one Li ion is moved to the neighboring vacancy of Li site. This path is not a suitable path for the Li ion in the Li_3N crystal reported by several experimental studies.

The Li_3N crystal has anisotropy of the Li ion conductivity and the conductivity along the c axis is much smaller than those in the a and b axes. Then we have used model clusters of the movement of the Li ion toward the c axis shown in Fig. 1.1 (iii) and (iv) for the comparison of the movement toward the different directions. Since there are several possibilities of the conduction path toward c axis, we have adopted two possible paths for the model clusters.

1.4.1.4 Local Cluster Energy of Mobile Li Ion

Figure 1.2a and b show the variation of the LCE with the different positions of the moving Li ion in the clusters (i) and (ii), respectively. In this figure, the ordinate

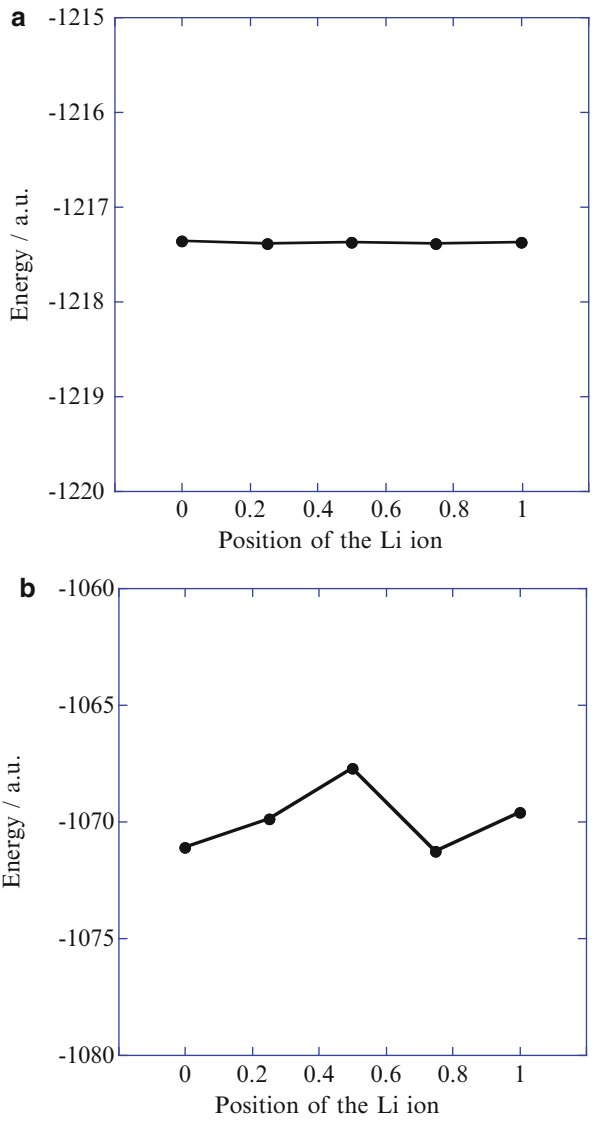

Fig. 1.2 The position dependence of total energy of the clusters, (**a**) cluster (i), (**b**) cluster (ii)

shows the LCE of the clusters in a.u. and the abscissa shows the relative position of the moving Li ion. In the case of cluster (i), the energy changes very small with the positions of the moving Li ion, that is, the difference between the minimum and the maximum is 0.031 a.u. This value is larger than the result of the band calculation (Sarnthein et al. 1996), since the LCE usually includes lager interaction with surface atoms. On the other hand, the energy change with the Li position in the cluster (ii) is 3.796 a.u. and is much larger than that in the cluster (i). Thus the LCE

evaluated by the Coulomb could be useful to discuss the movement of the Li ion in the Li ion conductors, although the cluster size, the number of sample points, the basis functions and the other computational parameters should be clarified to obtain the qualitative total energy of the cluster. Thus the Li ions on the Li_2N plane could move easier than those on the Li plane.

1.4.1.5 Bonding Nature and Li Ion Movement

The bonding state of the moving Li ions is analyzed, since the smaller energy different with the movement of the Li ion might be dependent on the chemical bonding of the moving Li ion.

Figure 1.3 shows net charge of the moving Li ions in clusters (i)–(iv). In this figure, the abscissa shows the relative position of the moving Li ion. Since the length of the conduction path (i)–(iv) are different, the value of 0 means the initial position and 1 means the final position of the moving Li ion so that the position of the moving lithium ion in each path is normalized.

In the cluster (i), shown as closed circles, the net charge is 0.41 at initial position. It changes little with the movement of the Li ion and becomes 0.43 at the final position. The charge of the Li ion is almost the same and no obvious changes are observed in the cluster (ii), shown as closed squares. In the Li_3N crystal, however, there is no obvious change of the net charge of the Li ion during the movement. In the cases of the clusters (iii) and (iv), shown as closed triangles and diamonds, the net charge of the Li ion at initial position is 0.28, which is clearly smaller than those in the clusters (i) and (ii). The net charge of the Li ion is increased at $x = 0.25$

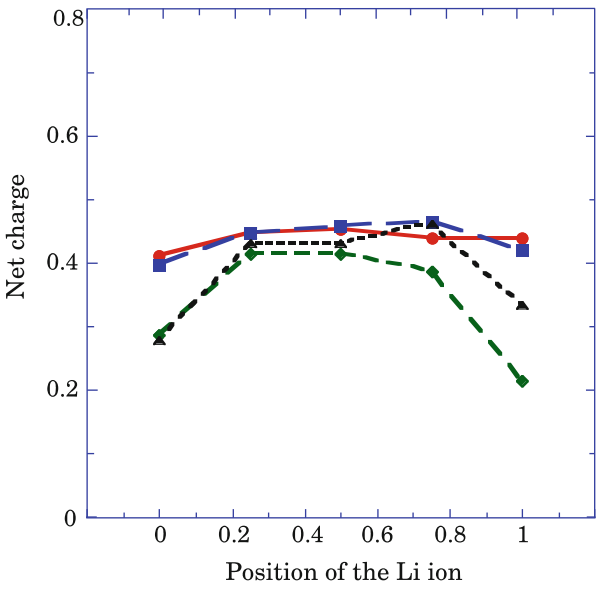

Fig. 1.3 The relationship between the net charge and the position of the moving Li ion in the model clusters (i)–(iv). ●: cluster (i), ■: cluster (ii), ▲: cluster (iii), ◆: cluster (iv)

and is almost constant until x = 0.75. At the final position the net charge becomes smaller again. This result might be caused by the structures of the model clusters. In the clusters (iii) and (iv), the initial and final positions are located on the surface of the model clusters. Though the surface atoms usually have larger electron density than the inner atoms, the net charges of the Li ions became smaller at the initial and the final positions in the clusters (iii) and (iv). There are some difficulties of the calculations of the conduction path along with the c axis because the cluster size becomes two times larger than the clusters (i) and (ii) if all the Li ions around the conduction path through the c axis are located inside of the model clusters. However, the net charge at the positions inside of the clusters, from x = 0.25 to x = 0.75, shows similar values as those observed in the clusters (i) and (ii).

Thus the net charges of the moving Li ions in the different paths are very similar each other and we can conclude that there is no obvious change of the ionic interaction of the moving Li ion in the experimentally reported conduction path compared with the other non-conduction paths.

Figure 1.4 shows the total bond overlap populations (TBOP) of the moving Li ion in the model clusters shown in Fig. 1.1. The TBOP means the summation of all the bond overlap populations between the moving Li ion and the surrounding ions, which shows the covalency of the bonding state of the moving Li ions.

In the cluster (i), which is the model of the Li_2N plane, TBOP is 0.82 at the initial position and is slightly decreased with the movement of the Li ion. There is a minimum of TBOP at x = 0.5. The TBOP is increased after x = 0.5 and is 0.79 at the final position. Basically the similar change is observed in the TBOP of the moving Li ion on the Li plane. In this plane the TBOP is 0.80 at the initial position and is decreased with the movement of the Li ion. A minimum of TBOP is observed at x = 0.5 and finally the TBOP becomes 0.78. At the initial and the final positions the

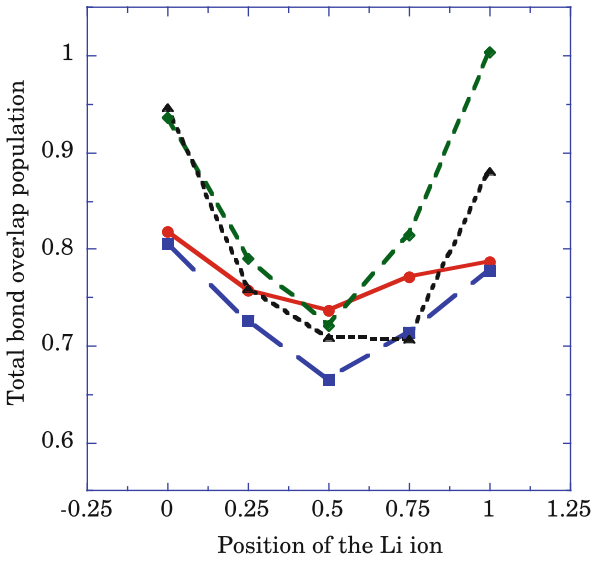

Fig. 1.4 The relationship between the total bond overlap population and the position of the moving Li ion in the model clusters (i)–(iv). ●: cluster (i), ■: cluster (ii), ▲: cluster (iii), ◆: cluster (iv)

TBOP of the moving Li ion on the Li_2N plane are almost the same as those on the Li plane. However, at the middle position, $x = 0.5$, the TBOP on the Li_2N plane is almost 0.1 larger than that on the Li plane. As the result, the difference between the maximum and the minimum of the TBOP of the Li ion on the Li_2N plane is 0.077, which is much smaller than that on the Li plane, 0.13. This smaller change of the TBOP through the path is a characteristic of the bonding nature of the moving Li ion on the Li_2N plane. Furthermore, this change is consistent with the results of the chemical bonding analyses.

In the case of the movement of the Li ion toward the c axis, the different changes are observed. In the model cluster (iii) for the c axis movement, the TBOP of the moving Li ion is 0.95 at the initial position. The TBOP of the moving Li ion is decreased largely with the movement and becomes minimum, 0.72, at $x = 0.5$. The change of the TBOP with the movement of the Li ion through the path toward the c axis is about 0.2, which is much larger than those in the clusters (i) and (ii). The same tendency is observed in the cluster (iv). The initial TBOP of the Li ion is 0.94 and the minimum is 0.70 at $x = 0.75$. The difference between the maximum and the minimum is 0.35. In general the surface ions have relatively large interaction with the surrounding ions. This "surface effect" is the reason of the large change of the covalency in these model clusters. However, since the net charge of the moving Li ion is almost the same as those on the Li and Li_2N plane in the positions in the range from $x = 0.25$ to 0.75 as shown in Fig. 1.3, the result suggests that surface effect of the bonding state of the moving Li ion could be neglect in these positions.

1.4.1.6 Conclusion

As the results, the variation of LCE with the movement of the Li ion suggests that the movement of the Li ion through the conduction path make the smaller energy change than another path. The net charge of the moving Li ion in any paths has very small change with the movement. Contrary to this, the variations of the total bond overlap populations of the moving Li ion are different from one another. Especially the TBOP of the Li ion changes smaller on the Li_2N plane, which contains the conduction path, than those on the other paths. The smaller change of TBOP of the moving Li ion is dependent on the little change of the BOP of both Li-Li and Li-N. These results suggest that the small change of the TBOP of the moving Li ion makes smaller energy difference with the movement and could be one of the origins of the fast movement of the Li ion in the Li_3N crystal.

1.4.2 Electronic States of Lanthanide Ions in Phosphate Glasses

1.4.2.1 Introduction

Rare-earth ion doped oxide glasses have been attractive for their application to white LED, the fiber-LASER amplification, and displays, etc. Many people have made effort to study about the absorption and luminescence spectra of these glassy materials (Miniscalco 1991; Wang et al. 1994; Souza et al. 2000; Reddy et al. 2000).

In these studies, theoretical analyses of the electronic state of rare-earth ions in oxide glasses are very important. Usually the absorption and fluorescence spectra of these glasses are analyzed by the empirical method (Ajithkumar et al. 2000; Tanabe et al. 2000, 2002; Jose et al. 2003; Moorthy et al. 2005). There are several empirical methods to analyze 4f-4f transition spectra of rare-earth ions. But in these methods, we need the experimental parameters to obtain the results.

Recently the relativistic DVME method, which is one of the first principles configuration interaction method is developed and there have been already many studies about electronic state of rare-earth ions in solid-state materials (Ishii et al. 2004a, b; Ogasawara et al. 2005; Watanabe et al. 2006; Toyoshima et al. 2007; Yoshida and Ogasawara 2009). However, there are few studies about fluorescence spectra of rare-earth ions in the oxide materials. We have calculated fluorescence spectra of the Pr^{3+} and Tb^{3+} ions in phosphate matrices by the relativistic DVME method. These phosphate materials have been expected as new laser materials for various applications because of their good fluorescence efficiency in the visible and infrared region.

1.4.2.2 Fluorescence Spectra of Pr^{3+} Ion in Phosphate Glass

Figure 1.5 shows model cluster, $H_{18}PrP_7O_{28}$, for the calculation of Pr^{3+} ions in the phosphate glasses used. This cluster includes seven surrounding PO_4 units terminated with H ions for the neutrality of the cluster. The atom positions are determined from $Pr(PO_3)_3$ crystal structure (Jouini et al. 2003). In this case, Madelung potential has not used for the calculation of the relativistic DV-Xα method. Though the cluster is a model cluster for $Pr(PO_3)_3$ crystal, it can be applied to the calculation of glassy materials because this model has no long-range structure.

Figure 1.6 shows the theoretical spectrum of the $H_{18}PrP_7O_{28}$ cluster. In the spectrum, the several initial states, such as $^3P_2$, $^3P_1$, $^3P_0$ and $^1I_6$, are used to obtain the theoretical fluorescence spectrum of Pr^{3+} ion in phosphate matrices. In this figure, the experimental Pr^{3+} fluorescence spectrum in the $Pr(PO_3)_3$ crystal is shown for comparison (Jouini et al. 2003). In the theoretical spectrum, there are two intense peaks around 350 and 570 nm. The peak positions shift slightly smaller

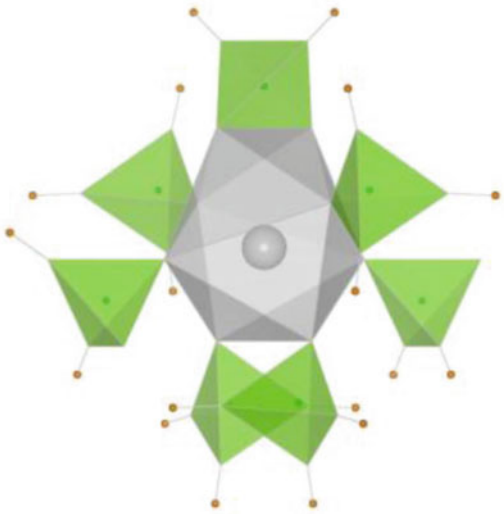

Fig. 1.5 Schematic diagram of the $H_{18}PrP_7O_{28}$ cluster

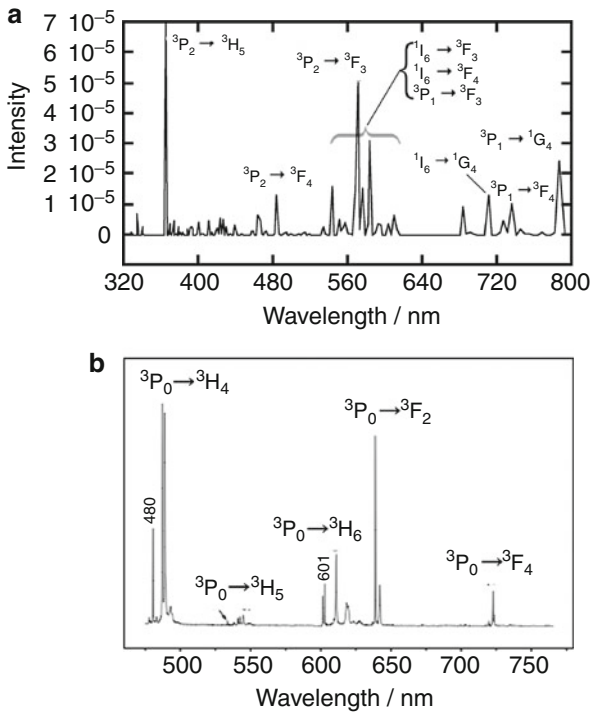

Fig. 1.6 Theoretical fluorescence spectrum of the $H_{18}PrP_7O_{28}$ cluster with several initial states. (**a**) Theoretical spectrum, (**b**) experimental spectrum reported by A. Jouini et al. 2003

wavelength but the relative positions of these major peaks are corresponding to those in the experimental spectrum. Furthermore, the relative peak intensities are also similar to those in the experimental spectrum. However, the assignments of the peaks shown in the figure are very complicated. For an example, the assignments of the intense peaks around 550–610 nm are several transitions from $^3P_2$, $^1I_6$, and $^3P_1$ to $^3F_3$, and from $^1I_6$ to $^3F_4$, though the corresponding peaks around 600–650 nm in the experimental spectrum are assigned to the transitions from $^3P_0$ to $^3H_6$ and $^3F_2$. This result suggests that there are several initial states in the fluorescence of Pr^{3+} ion in phosphate matrices, and it is very difficult to make assignment of the peaks by only the empirical method. This result also shows the relativistic DVME method is very useful to analyze fluorescence spectra of rare-earth ions in phosphate matrices and the first principles calculation is necessary to analyze the fluorescence spectra of rare-earth ions.

1.4.2.3 Fluorescence Spectra of Tb^{3+} Ion in Phosphate Glass

Figure 1.7 shows model clusters, $H_{15}TbP_6O_{24}$, used in the calculation of the electronic state of the Tb^{3+} ion. In this model cluster the atom positions are estimated by the ionic radii of Tb^{3+} ion and the structure of $Lu(PO_3)_3$ crystal, since there is no report about the crystal structure of Terbium phosphate crystals (Yuan et al. 2008). The crystal structure of $Lu(PO_3)_3$ is monoclinic, space group C_C and cell parameters $a = 13.972$ Å, $b = 20.018$ Å, $c = 9.9556$ Å, $\beta = 127.351°$. The model cluster includes only one lanthanide ion site. This cluster includes six surrounding PO_4 units terminated with H ions for the neutrality of the cluster, though the cluster of the Pr^{3+} ion, which is a heavy-lanthanide, has seven PO_4 units.

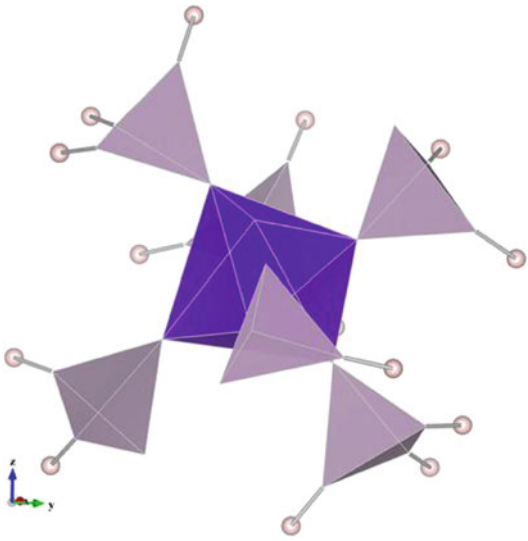

Fig. 1.7 Schematic diagram of the $H_{18}TbP_7O_{28}$ cluster (These figures were drawn with VESTA developed by K. Momma and F. Izumi)

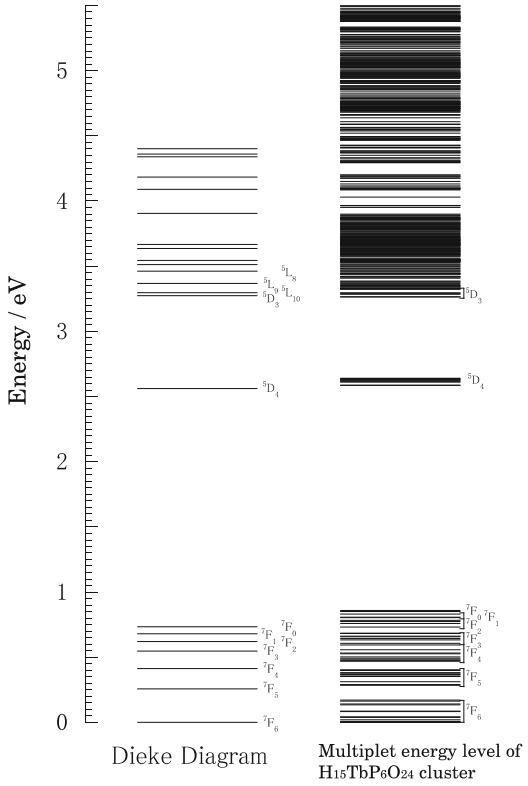

Fig. 1.8 Multiplet energy level structure of $H_{18}TbP_7O_{28}$

Figure 1.8 shows the obtained multiplet level structure of the Tb^{3+} ion in the $H_{15}TbP_6O_{24}$ cluster. Tough there are only 14 molecular orbitals mainly contributed by 4f atomic orbitals of the Tb^{3+} ion in the usual one electron approximation molecular orbital method, there are 3,003 multiplet levels after the electron configuration interaction calculation. The level structure of the multiplet states is basically corresponding to that reported by Dieke (1968).

Figure 1.9 shows the calculated and experimental absorption spectra of the Tb^{3+} ion in the $H_{15}TbP_6O_{24}$ cluster. The experimental spectrum is the result of the Tb^{3+} ion doped calcium meta-phosphate glass, which is prepared to compare with the theoretical ones.

In the relativistic DVME method, the energy of the multiplet levels in the 4f-4f transitions is usually over estimated (Brik and Ogasawara 2007). In these theoretical spectra, the energy scale is corrected with a factor, 0.75 for easiness of comparison.

In the experimental spectra, there are small peaks at about 2.51 in the visible region. The same peak is observed in the theoretical spectra and the main components of this peak is the transition from $^5D_4$ to $^7F_6$. Basically, the peak position observed in the theoretical spectrum is in good agreement with the experimental one. Thus, relativistic DVME method is useful to assign the peaks in the absorption spectra of Tb^{3+} ion in phosphate glasses.

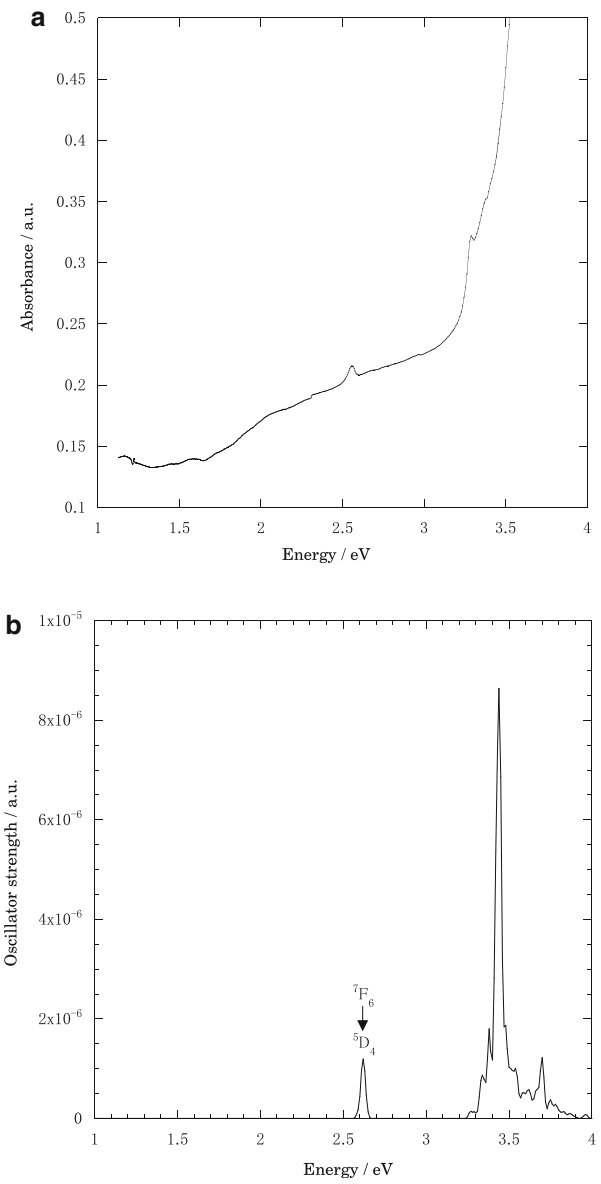

Fig. 1.9 Absorption spectra of $H_{18}TbP_7O_{28}$. The experimental spectra were measurements of the $50CaO•50P_2O_5$ glass with 1 mol% of Tb_2O_3. (**a**) Experimental spectrum, (**b**) theoretical spectrum

Figure 1.10a is the experimental fluorescence spectrum of Tb^{3+} doped $50P_2O_5•50CaO$ glass under excitation with 3.29 eV. In this spectrum, two intense peaks around 1.58 and 3.32 eV are reflection of the excitation light. There is an intense peak at 2.29 eV and another at 2.54 eV. These peaks are assigned to the transition from $^5D_4$ to $^7F_5$ and from $^5D_4$ to $^7F_4$, respectively, by referring the Dieke diagram. The other small peaks are observed at 2.00, 2.12, 2.71, 2.85 and 3.00 eV,

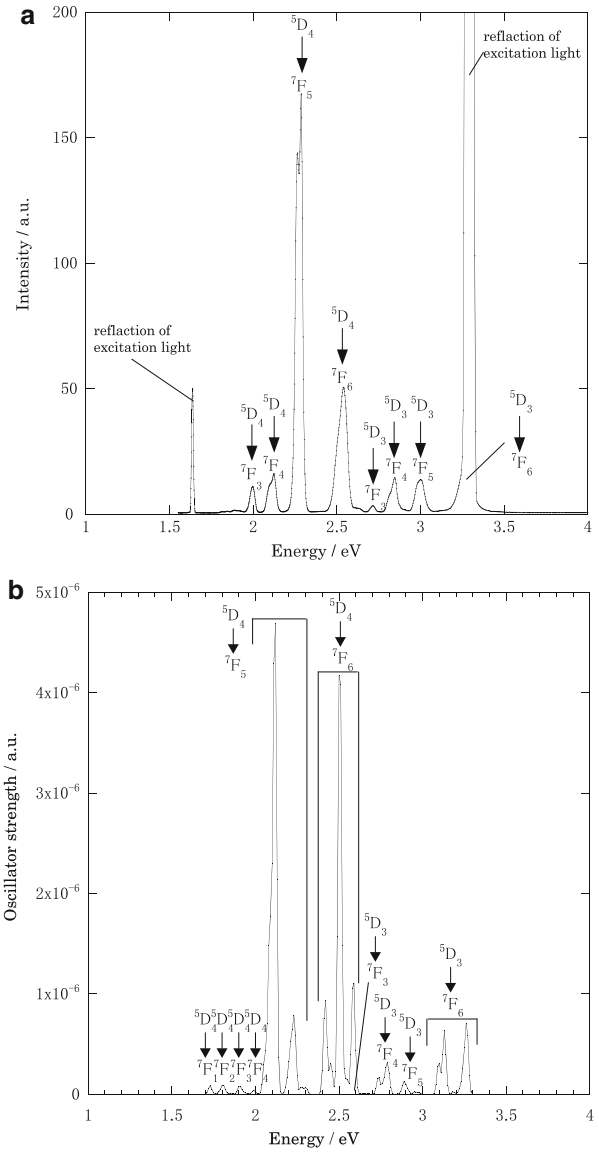

Fig. 1.10 Fluorescence spectra of $H_{18}TbP_7O_{28}$. (**a**) Experimental spectrum, (**b**) theoretical spectrum of Tb^{3+} ion doped $50CaO{\bullet}50P_2O_5$ glass

whose assignments are described in the figure. Figure 1.10b shows the theoretical spectrum of the $H_{15}TbP_6O_{24}$ cluster. In the spectrum, there are two intense peaks around 2.12 and 2.51 eV; those are corresponding to the peaks from $^5D_4$ to $^7F_5$ and from $^5D_4$ to $^7F_6$ in the experimental ones, respectively. The peaks observed in the experimental spectra are usually assigned by referring the Dieke diagram, so that the assignments are sometime incorrect especially in the spectra in the lanthanide ions with the complex multiplet energy levels. In the case of the Pr^{3+} ion, the